



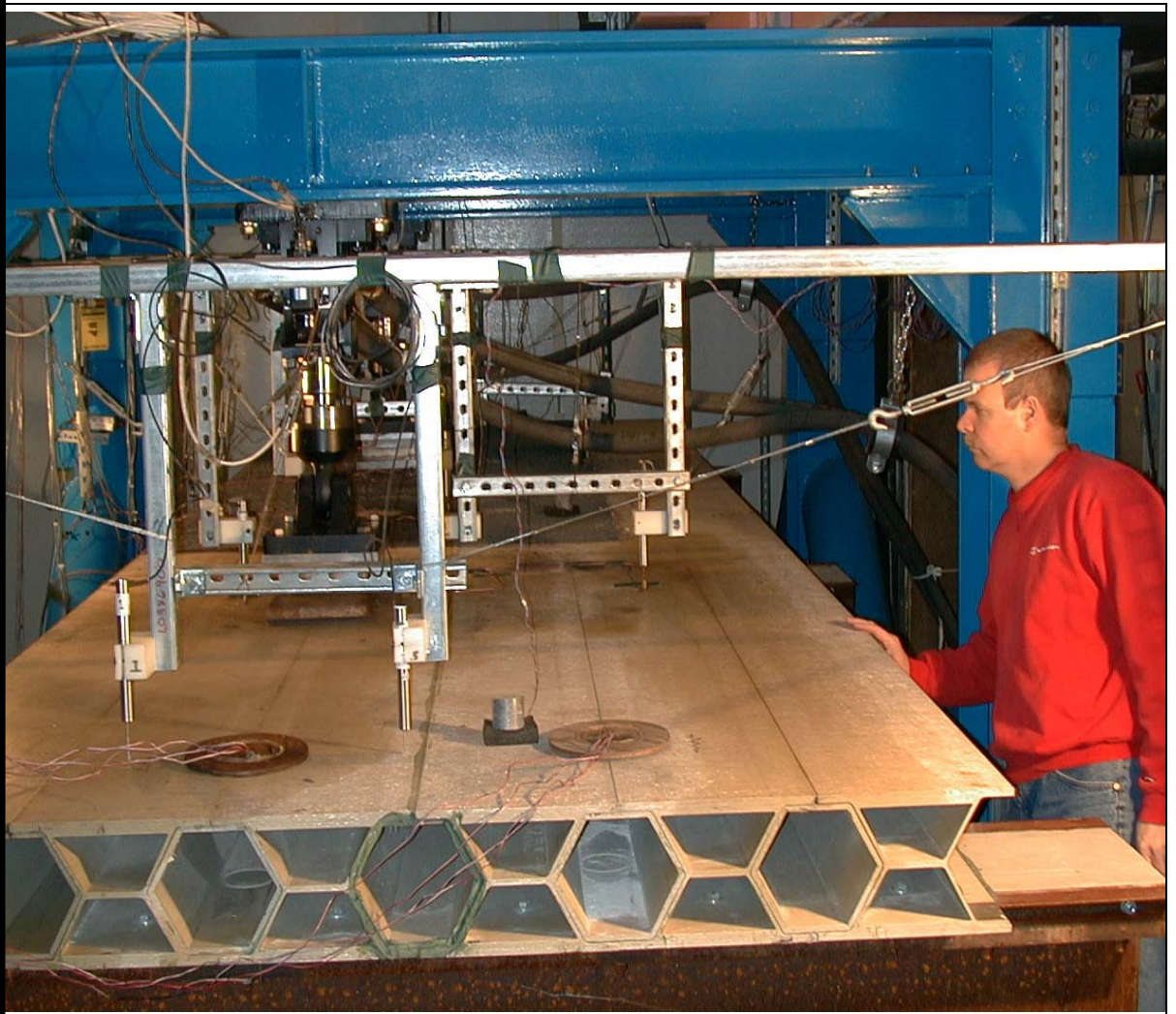
US Army Corps  
of Engineers®

Engineer Research and  
Development Center

# FATIGUE EVALUATION OF MULTIPLE FIBER-REINFORCED POLYMER BRIDGE DECK SYSTEMS OVER EXISTING GIRDERS PHASE II REPORT

Piyush K. Dutta, Roberto Lopez-Anido  
Soon -Chul Kwon and Glenn D. Durell

November 2003



**FATIGUE EVALUATION OF MULTIPLE FIBER-REINFORCED  
POLYMER BRIDGE DECK SYSTEMS OVER EXISTING GIRDERS-  
PHASE II REPORT**

**Piyush K. Dutta<sup>1</sup>**

**Roberto Lopez-Anido<sup>2</sup>**

**Soon-Chul Kwon<sup>1</sup>**

**Glenn D. Durell**

<sup>1</sup> US Army Cold Regions Research and Engineering Laboratory, ERDC, Hanover, NH

<sup>2</sup> Department of Civil and Environmental Engineering, and Advanced Engineered Wood  
Composites Center, University of Maine, Orono, ME

November 2003

Prepared in cooperation with the Ohio Department of Transportation and  
the U.S. Department of Transportation, Federal Highway Administration

## FATIGUE EVALUATION OF MULTIPLE FIBER-REINFORCED POLYMER BRIDGE DECK SYSTEMS OVER EXISTING GIRDERS-PHASE II

---

**Piyush K. Dutta, Roberto Lopez-Anido , Soon-Chul Kwon and Glenn D. Durell**

### **ABSTRACT**

Decks manufactured with fiber-reinforced polymer (FRP) composite materials are used in highway bridges. A performance evaluation of FRP composite decks subjected to simulated traffic loads that induce repetitive stress cycles under extremely high and low temperature is presented. Fatigue testing of three FRP composite bridge deck prototypes and one FRP-concrete hybrid bridge deck prototype under two extreme temperature conditions:  $-30^{\circ}\text{C}$  ( $-22^{\circ}\text{F}$ ), and  $50^{\circ}\text{C}$  ( $122^{\circ}\text{F}$ ) was conducted. The fatigue response of the deck prototypes was correlated with the baseline performance of a conventional reinforced concrete deck subjected to similar test conditions. Design loads were applied simultaneously at two points using servo-controlled hydraulic actuators specially designed and fabricated to perform under extreme temperatures. Quasi-static load-deflection and load-strain characteristics were determined at predetermined fatigue cycle levels. No significant distress was observed in any of the composite deck prototypes during ten million load cycles. The effects of extreme temperatures and accumulated load cycles on the load-deflection and load-strain response of FRP composite and FRP-concrete hybrid bridge decks are discussed based on the experimental results.

## TABLE OF CONTENTS

ABSTRACT .....	3
LIST OF TABLES .....	5
LIST OF FIGURES .....	5
1. INTRODUCTION .....	6
2. COMPOSITE DECK PROTOTYPES.....	7
2.1 Conventional Reinforced-Concrete Bridge Deck System .....	7
2.2 Hybrid FRP–Concrete Bridge Deck System.....	7
2.3 FRP Bridge Deck Fabricated by the VARTM Process.....	7
2.4 FRP Bridge Deck System Fabricated by the Pultrusion Process.....	7
2.5 FRP Bridge Deck Fabricated by the Contact Molding Hand Lay-Up Process.....	8
3. EXPERIMENTAL SETUP.....	8
3.1 Self-Reacting Loading Frame .....	8
3.2 Instrumentation .....	8
4. FATIGUE TEST PROCEDURE .....	8
5. DISCUSSION OF EXPERIMENTAL RESULTS.....	9
6. CONCLUSIONS.....	10
7. ACKNOWLEDGEMENTS .....	10
8. REFERENCES .....	11

## LIST OF TABLES

Table 1. FRP Composite Deck Prototypes .....	12
Table 2. Deflections and strains at maximum load after 10 million cycles .....	13

## LIST OF FIGURES

Figure 1. View of FRP deck prototypes on steel girders .....	14
Figure 2. Cross-section of FRP deck systems.....	15
Figure 3. Experimental setup: (a) Self-reacting test frame for fatigue loading; (b) Instrumented deck prototype.....	16
Figure 4. Instrumentation and loading: (a) LVDTs, thermocouples and strain gages; (b) Hydraulic actuator and loading pad .....	17
Figure 5. Test setup and instrumentation layout.....	18
Figure 6. Load cycling and temperature history.....	19
Figure 7. Typical quasi-static load test .....	20
Figure 8. Load–deflection curves after ten million cycles of fatigue loading: (a) Bridge #1; (b) Bridge #2; (c) Bridge #3; (d) Bridge #4; (e) Bridge #5 .....	21
Figure 9. Load–deflection curves at location LV-2 for increasing load cycles: (a) Bridge #1; (b) Bridge #2; (c) Bridge #3; (d) Bridge #4; (e) Bridge #5 .....	22
Figure 10. Effects of temperature on the load-deflection response at location LV-2 for 10 million fatigue load cycles: (a) Low temperature; (b) High temperature.....	23
Figure 11. Load–Strain curves for deck prototypes: (a) Low temperature; (b) High temperature.....	24
Figure 12. Comparison of deflections at maximum load after 10 million cycles at location LV-2 .....	25
Figure 13. Comparison of strains at maximum load after 10 million cycles at location SG-2.....	26

## 1. INTRODUCTION

Of all elements in a bridge superstructure, bridge decks may perhaps require the maximum maintenance, for reasons ranging from the deterioration of the wearing surface to the degradation of the deck system itself. Added to the problems of deterioration are the issues related to the need for higher load ratings (HS20 to HS25, for example) and increased number of lanes to accommodate the ever-increasing traffic flow on major arteries (Lopez-Anido and Karbhari 1990). Beyond the costs and visible consequences associated with continuous retrofit and repair of such structural components are the real consequences related to losses in productivity and overall economies related to time and resources caused by delays and detours (See for example, Ehelen and Marshall, 1996). Reasons such as those listed above provide significant impetus for the development of new bridge decks out of materials that are durable, light and easy to install. Besides the potentially lower overall life-cycle costs (due to decreased maintenance requirements), decks fabricated from fiber reinforced composites are significantly lighter, thereby affecting savings in substructure costs, enabling the use of higher live load levels in the case of replacement decks, and bringing forth the potential of longer unsupported spans and enhanced seismic resistance. However, the response of FRP composite decks to fatigue loading in extreme temperatures has not been studied extensively (Lopez-Anido et al. 1998, 1999; Kwon et al. 2001).

An evaluation plan for FRP bridge decks has been recently proposed by the HITEC program (Karbhari 2000). The panel has identified key technical issues and proposed performance verification tests related to: a) Structural system response, inspection, maintenance and repair; b) Joints and connections; and c) Materials and manufacturing. The Federal Highway Administration and the Ohio Department of Transportation is conducting an evaluation program for four different FRP bridge deck systems, which ranges from durability characterization and structural fatigue testing to field installation and monitoring (Triandafilou 2000). Preliminary fatigue test results were reported (Lopez-Anido et al. 2001).

In this study, experimental fatigue evaluation of five deck prototypes, which included three full-size FRP composite bridge decks, one hybrid FRP-concrete deck, and one reinforced-concrete conventional bridge deck, was conducted (See Figure 1 and Table 1). The deck prototypes were evaluated under two extreme temperatures to assess the fatigue-temperature response. Each deck prototype was initially subjected to one million simulated wheel load cycles at low temperature,  $-30^{\circ}\text{C}$  ( $-22^{\circ}\text{F}$ ), and another one million cycles at a controlled high temperature,  $50^{\circ}\text{C}$  ( $122^{\circ}\text{F}$ ). The results of these initial tests were presented by Lopez-Anido et al. (2001). The results presented in this paper correspond to testing each deck prototype for an additional four million cycles at low temperature and four million cycles at high temperature. Besides, three different polymer concrete wearing surfaces, each  $3.7 \times 0.45 \text{ m}$  ( $144 \times 18 \text{ in}$ ) and  $13 \text{ to } 19 \text{ mm}$  ( $0.5 \text{ to } 0.75 \text{ in}$ ), from three different vendors were provided on each of the three FRP composite bridge decks.

Quasi-static load tests were conducted at specific intervals during fatigue cycling to evaluate the load-deflection and load-strain responses at several deck locations. The experimental results were correlated with the performance of a conventional reinforced-concrete deck subjected to the same series of tests.

## 2. COMPOSITE DECK PROTOTYPES

### 2.1 Conventional Reinforced-Concrete Bridge Deck System

The conventional reinforced-concrete deck (Bridge #1) was designed by the Ohio Department of Transportation (ODOT) for the benchmark response of the set of FRP bridge decks. This deck prototype had dimensions of  $1.828 \times 6.100 \times 0.178$  m ( $72 \times 240 \times 7$  in.) and was connected to the supporting W36x182 steel girders using shear studs. In the direction perpendicular to the girders, top steel reinforcing bars (No. 5) were placed in the concrete slab with a spacing of 133 mm (5.25 in.) and a cover of 38 mm (1.5 in.). A bottom reinforcement layer was placed with a spacing of 152-mm (6-in.). In the direction parallel to the girders, top distribution reinforcement (No. 4 bar) and bottom distribution reinforcement (No. 5 bar) was used. The concrete compressive strength was 29.3 MPa (4250 psi).

### 2.2 Hybrid FRP–Concrete Bridge Deck System

The hybrid FRP-concrete deck system (Bridge #2) had FRP pultruded panels that were used for stay-in-place formwork and concrete reinforcement (Figure 2). The pultruded panels had a width of 457 mm (18 in.) and two stiffening tubular cells with a height of 76 mm (3 in.). This FRP composite material was reinforced with E-glass roving and directional-bias fabric in a polyester-vinyl ester resin blend.

Concrete was cast on the FRP composite panels to attain the specified slab depth of 203 mm (8 in.). Top reinforcement in both directions was provided by non-corrosive E-glass rebar with deformations to improve the bond with the concrete. The deck was connected to the supporting steel girders using shear studs. After placing the pultruded panels on the steel girders, shear studs were welded. This test specimen had dimensions of  $1.828 \times 6.100 \times 0.203$  m ( $72 \times 240 \times 8$  in.). A concrete haunch was placed between the FRP deck panels and the steel girders.

### 2.3 FRP Bridge Deck Fabricated by the VARTM Process

Bridge #3 was fabricated by the VARTM (Vacuum Assisted Resin Transfer Molding) process (Figure 2). The deck was composed of face sheets reinforced with multi-axial stitched E-glass fabric (0/90/±45) (BTI, QM6408), and an integral cell core that was wrapped with an E-glass fabric. The resin matrix was vinyl ester resin (Dow Derakane 411). The deck prototype had dimensions of  $1.828 \times 6.100 \times 0.203$  m ( $72 \times 240 \times 8$  in.). Two panels of 0.914 m (36 in.) in width and 6.100 m (240 in.) in length were connected with a longitudinal joint (perpendicular to the girder direction) to form the deck prototype while providing a smooth surface.

### 2.4 FRP Bridge Deck System Fabricated by the Pultrusion Process

Bridge #4 was made of FRP composite profiles with constant cross-section fabricated by the pultrusion process (Figure 2). In a second operation the components are interlocked and bonded using a toughened adhesive. In this way large panels can be fabricated and shipped to the construction site. This deck is typically highly orthotropic with the main stiffness direction corresponding to the axis of the pultruded profiles, which was perpendicular to the supporting girder direction. The cross-section was composed of hexagonal and double trapezoidal profiles (Lopez-Anido et al. 2001).

The deck prototype dimensions were  $1.828 \times 6.100 \times 0.203$  m ( $72 \times 240 \times 8$  in.). The fiber reinforcement was E-glass continuous roving and multi-axial stitched E-glass fabric (90/±45) (BTI, TH4000 / THX1501). The resin matrix was vinyl ester (Reichhold, Atlac 580-05),

## **2.5 FRP Bridge Deck Fabricated by the Contact Molding Hand Lay-Up Process**

Bridge #5 was fabricated based on the concept of sandwich construction using a low-density honeycomb core sandwiched between two contact-molded hand lay-up face sheets (Figure 2). The dimensions of the deck prototype were  $1.828 \times 6.100 \times 0.203$  m ( $72 \times 240 \times 8$  in.). The resin matrix was made of isophthalic / terephthalic polymer resin (AOC, Vibrin F457-BRP-25), which was reinforced with bi-axial E-glass fabric (0/90) and mat (BTI, CM4810 & CCC A118).

## **3. EXPERIMENTAL SETUP**

### **3.1 Self-Reacting Loading Frame**

Each deck prototype was placed on three W36x182 steel girders, resulting in a continuous two-span bridge structure Figure 3. A self-reacting steel test frame was designed for a maximum load capacity of 270 kN (60,000 lb). The maximum deflection of the steel transverse beam was limited to less than 0.25 mm (0.01 in.). Two actuators mounted on the two cross arms of this load frame applied the load through two steel plates of  $228 \times 559$  mm ( $9 \times 22$  in.) centered with respect to the supports of the span, which simulate the AASHTO HS20-44 design truck wheel load print. The long dimension of the plate was perpendicular to the girder direction. The inner long edge of the plate was 178 mm (7 in.) away from the center of the deck. An elastomeric pad was placed between each steel plate and the prototypes to provide uniform pressure that simulates the wheel load action (Figure 4). The setup induced a positive bending moment under the load and a negative bending moment on the central support.

### **3.2 Instrumentation**

Each test deck was instrumented with strain gages (EA-5-500BL-350, Micro-Measurements), thermocouples, and linear voltage differential transducers (LVDTs), which were supported by an independent steel frame. The LVDTs were used to measure deflections on the top and bottom surfaces of the decks. Seven thermocouples were used on four sides of each deck, and one thermocouple was used for ambient temperature (Figure 4). The locations of the strain gages bonded to the bottom deck surface were symmetrical with respect to the numerically matching strain gages bonded to the top surface of decks. The complete instrumentation layout is shown in Figure 5.

## **4. FATIGUE TEST PROCEDURE**

The fatigue evaluation procedure consisted of applying four million simulated wheel load cycles at  $-30^{\circ}\text{C}$  ( $-22^{\circ}\text{F}$ ) and another four million cycles at  $50^{\circ}\text{C}$  ( $122^{\circ}\text{F}$ ) (See Figure 6). The fatigue performance of each FRP deck prototype was compared with the response of the conventional reinforced-concrete deck. The fatigue load range was computed for an AASHTO HS20-44 truck wheel with impact and dead load. A computed load of 115 kN (26,000 lb) was applied

simultaneously at two points by servo-controlled hydraulic actuators specially designed and fabricated for this study

The maximum applied load ( $P_{\max}$ ) was 115 kN (26,000 lb). The minimum applied load ( $P_{\min}$ ) was 9 kN (2,000 lb). Therefore, the fatigue stress ratio ( $R = P_{\min}/P_{\max}$ ) was 0.077. Loading was applied using a sinusoidal waveform with a frequency of 3.5 Hz.

Initially a quasi-static test was performed at room temperature. Then the testing room temperature was changed by operating either the refrigeration system for cooling or operating the heating system for raising the temperature of the room. Once the equilibrium temperature for the deck was achieved fatigue load cycling was initiated.

Quasi-static load deflection tests were performed at regular intervals. In the quasi-static test the load was applied at a rate of 1 mm/min. (0.04 in./min) and sensor measurements were recorded every 3 seconds. Each quasi-static test consisted of a loading and unloading cycle and was repeated three times, as shown in Figure 7.

## 5. DISCUSSION OF EXPERIMENTAL RESULTS

Fatigue damage accumulation can induce stiffness degradation of the FRP composite deck material. Fatigue damage can also lead to residual deformation in the deck and in the deck-girder haunch connections. Thus, the fatigue performance evaluation was based on assessing the residual stiffness of the deck response and the fatigue damage. Quasi-static load deflection tests were conducted for damage assessment. The experimental data were analyzed and load-deflection curves were generated.

The FRP deck prototypes did not fail during the loading cycles. However, following the ten million cycles of loading at two extreme temperatures, degradation of stiffness was observed (Figure 8 and Figure 9).

The load-deflection curves for the low temperature,  $-30^{\circ}\text{C}$  ( $-22^{\circ}\text{F}$ ), and the high temperature,  $50^{\circ}\text{C}$  ( $122^{\circ}\text{F}$ ), at the five LVDT locations on the top of each panel and aligned in the direction perpendicular to girders are shown in Figure 8. The reinforced-concrete deck (Bridge #1) and the FRP-concrete hybrid deck (Bridge #2) exhibited higher stiffness than the FRP composite decks (Bridges #3, #4, and #5).

Load deflection curves for each deck prototype for the LVDT position LV-2 before fatigue cycling, after 2 million load cycles and after 10 million load cycles are shown in Figure 9. The decrease in slope of the load-deflection curves with number of fatigue cycles, indicate damage accumulation in the decks.

The effects of temperature on the load-deflection response are presented in Figure 10. As expected, the deck stiffness was reduced at the higher temperature level. The reduction in stiffness with temperature was more important for the FRP composite decks than for the reinforced-concrete deck and the FRP-concrete deck. From the maximum load-deflection curves (Figure 10), it was observed that the FRP bridge deck fabricated by the VARTM process (Bridge #3) and the FRP bridge deck fabricated by the pultrusion process (Bridge #4) had significantly more deflection than that of reinforced-concrete deck (Bridge #1) and the FRP-composite hybrid deck (Bridge #2). There was only a relatively small change in deck stiffness between the FRP bridge deck fabricated by the hand lay-up contact molding process (Bridge #5) and the reinforced-concrete bridge deck (Bridge #1) at both low and high temperatures.

Low-temperature and high-temperature load-strain curves were obtained from the strain gage SG-2 measurements, as shown in Figure 11. The curves for the deck prototype at each temperature level indicate that there was a significant difference in strain between the FRP composite decks and the reinforced-concrete deck. However, there was almost no difference in the load-strain response between the FRP composite bridge deck fabricated by the pultrusion process (Bridge #4) and the FRP bridge deck fabricated by the VARTM process (Bridge #3). The hybrid FRP-concrete bridge deck (Bridge #2) was stiffer (higher load-strain slope) than the reinforced-concrete deck (Bridge #1), as shown in Figure 11. This difference is attributed to the greater thickness of the hybrid FRP-concrete deck compared to the reinforced-concrete deck. Comparisons of deflections and strains corresponding to the maximum load for the five bridge deck prototypes after 10 million load cycles are presented in Figures 12 and 13. A summary of deflections and strain values at maximum load is also provided in Table 2.

The significant stiffness change with temperature implies that the deck stiffness was controlled mainly by temperature changes and not by the number of applied load cycles. The deck prototypes were inspected visually for signs of distress, such as cracks and damage at connections after fatigue cycling. No damage was visible in the three FRP composite decks (Bridge #3, Bridge #4, and Bridge #5), nor any cracks or delaminations were visible in any of the three polymer concrete wearing surfaces. However, hairline cracks were observed in the tension region over the FRP-concrete hybrid deck (Bridge #2).

## 6. CONCLUSIONS

The general conclusions drawn from the results of the investigation are:

1. A protocol for fatigue performance evaluation of FRP composite bridge deck prototypes under extreme temperatures was implemented.
2. A correlation with a benchmark conventional reinforced concrete deck was established.
3. The load-deflection response (stiffness) of the FRP composite decks was significantly affected by extreme temperature levels.
4. Progressive degradation in stiffness with load cycling was observed at high temperature, 50°C (122°F), testing condition for all deck prototypes. At low temperature, -30°C (-22°F), reduction of stiffness with load cycling was not as significant.

## 7. ACKNOWLEDGEMENTS

This work was sponsored by the Federal Highway Administration and the Ohio Department of Transportation through a contract with the University of Cincinnati. The authors thank John Bouzon, Thomas Tantillo, Jeffrey Stark, Rosanne Stoops, and John Gagnon for the experimental setup and assistance during testing. Steve Morton, previously with the Ohio DOT, provided test planning and inspiration for the work.

## 8. REFERENCES

1. American Association of State Highway and Transportation Officials (1998). “LRFD Design Specifications,” Washington, D.C.
2. Ehelen, M. A., and Marshall, H. E., (1996). *The Economics of New-Technology Materials in Construction: A Case Study of FRP Composite Bridge Decking*, Report NISTIR 5864, National Institute of Standards and Technology, Gaithersburg, MD.
3. Karbhari, V., (2000) FRP Bridge Decks Evaluation Panel, *FRP Composite Bridge Decks*, HITEC Evaluation Plan Civil, Engineering Research Foundation, Washington, DC.
4. Kwon, SCh., Dutta, P., Hui, D., and Kim, Y.H. (2001). “Thermal Performance Evaluation of Fiber Reinforced Polymer (FRP) Deck Systems over a Wide Temperature Range,” Int. Conf on Composite Engineering, Tenerife, Canary Islands, Spain, pp 507–510.
5. Lopez-Anido, R, Stephenson, LD, and Howdyshell, P. (1998). “Durability of Modular FRP Composite Bridge Deck under Cyclic Loading, Durability of FRP Composites for Construction,” *Durability of FRP Composites for Construction*, Eds. B. Benmokrane and H. Rahman, Sherbrooke, Canada, pp. 611–622.
6. Lopez-Anido, R, Dutta, P, Morton, S, Shahrooz, B, and Harik, I (1999). “Evaluation of FRP Bridge Deck System on Steel Girders: Fatigue and Durability,” SAMPE-99 Conference, Long Beach, California.
7. Lopez-Anido, R. and Karbhari, V.M. (2000). Chapter 2: “Fiber Reinforced Composites in Civil Infrastructure,” in *Emerging Materials for Civil Engineering Infrastructure - State of the Art*, Edited by Lopez-Anido, R.A. and Naik, T.R., peer-reviewed, pp. 41-78, ASCE Press, Reston, VA.
8. Lopez-Anido, R, Harik, I, Dutta, P, and Shahrooz, B (2001). “Field Performance Evaluation of Multiple Fiber-Reinforced Polymer Bridge Deck Systems over Existing Girders—Phase 1,” Ohio Department of Transportation, Columbus, Ohio.
9. Triandafilou, L., (2000), “The Great Miami FRP Composite Bridge Deck Project”, Report by the Federal Highway Administration - Eastern Resource Center, Presented at the 5th World Pultrusion Conference, European Pultrusion Technology Association, Berlin.

**Table 1. FRP Composite Deck Prototypes**

Deck No.	Deck Material	Dimensions (mm)	Fabrication Process	Resin Matrix	Reinforcements
Bridge #1	Conventional Reinforced-Concrete	1,829×6,096×179	N.A.		
Bridge #2	Hybrid FRP-Concrete (stay-in-place formwork)	1,829×6,096×203	Cast-In-Place Concrete	Polyester-Vinyl ester	E-glass Roving/ Directional-bias Fabric
Bridge #3	FRP composite (sandwich construction)	1,829×6,096×203	VARTM	Vinyl ester	Multi-Axial Stitched E-glass fabric/ Integral cell core
Bridge #4	FRP composite (interlocking profiles)	1,829×6,096×203	Pultrusion	Vinyl ester	E-glass Continuous Roving/ Multi-Axial Stitched E-glass fabric
Bridge #5	FRP composite (sandwich construction)	1,829×6,096×203	Contact Molding Hand-Lay up	Isophthalic /Terephthalic polymer	Honeycomb Core/ Biaxial E-glass Fabric and mat

**Table 2. Deflections and strains at maximum load after 10 million cycles**

Bridge No.	Deflection (mm) at location LV-2			Strain (micro-strains) at location SG-2		
	Low Temperature	High Temperature	Change %	Low Temperature	High Temperature	Change %
Bridge #1	2.05	2.17	5.9	231	248	7.8
Bridge #2	1.48	2.13	43.6	117	139	18.5
Bridge #3	3.28	3.48	6.2	534	574	7.6
Bridge #4	3.43	4.08	18.8	503	564	12.1
Bridge #5	2.18	2.42	10.9	391	446	14.3



**Figure 1. View of FRP deck prototypes on steel girders**

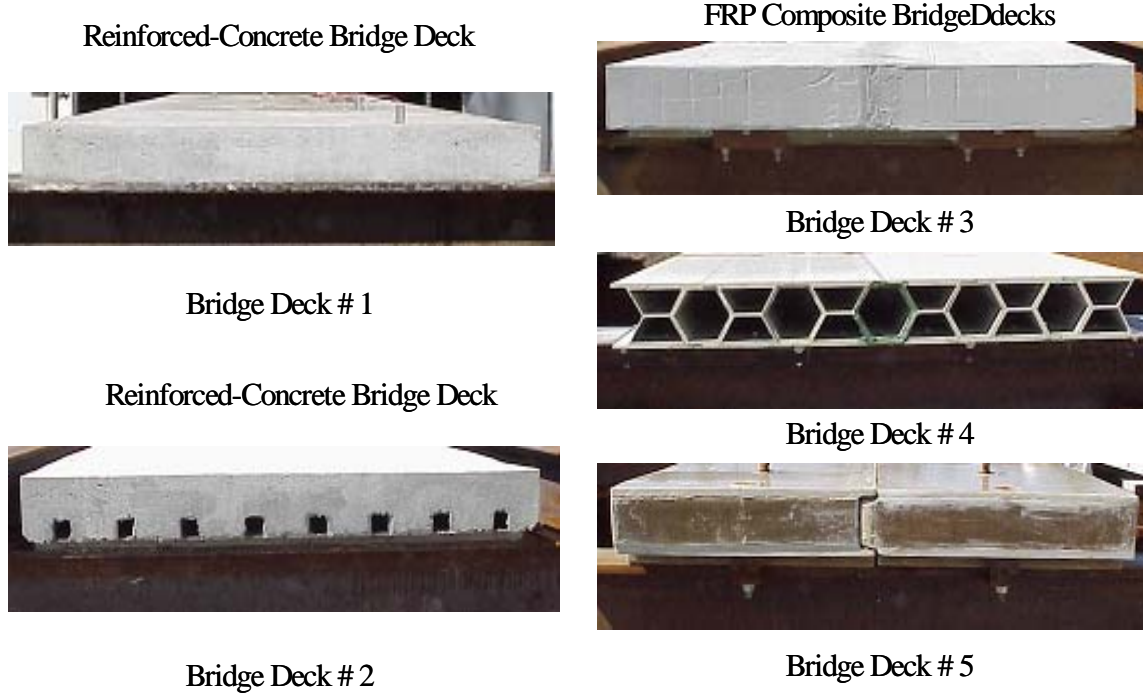
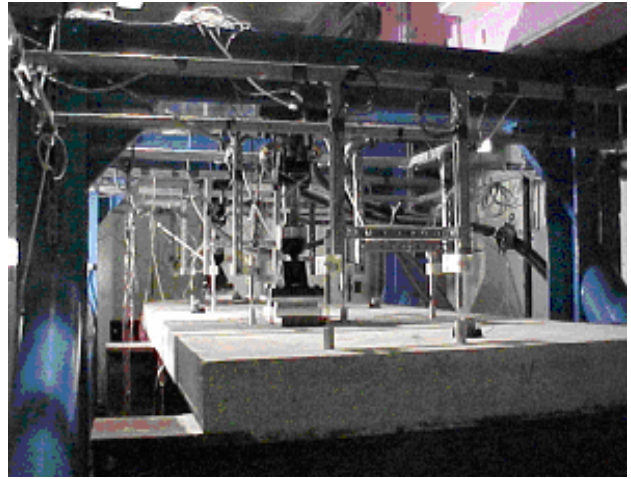


**Figure 2. Cross-section of FRP deck systems**

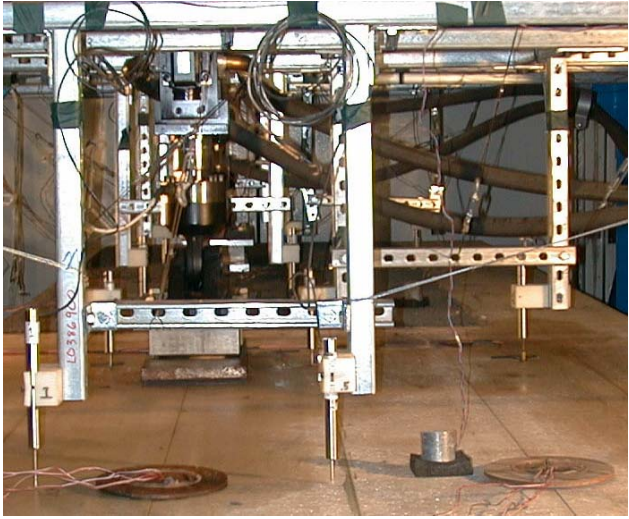


(a)



(b)

**Figure 3. Experimental setup: (a) Self-reacting test frame for fatigue loading; (b) Instrumented deck prototype**



(a)



(b)

**Figure 4. Instrumentation and loading: (a) LVDTs, thermocouples and strain gages; (b) Hydraulic actuator and loading pad**

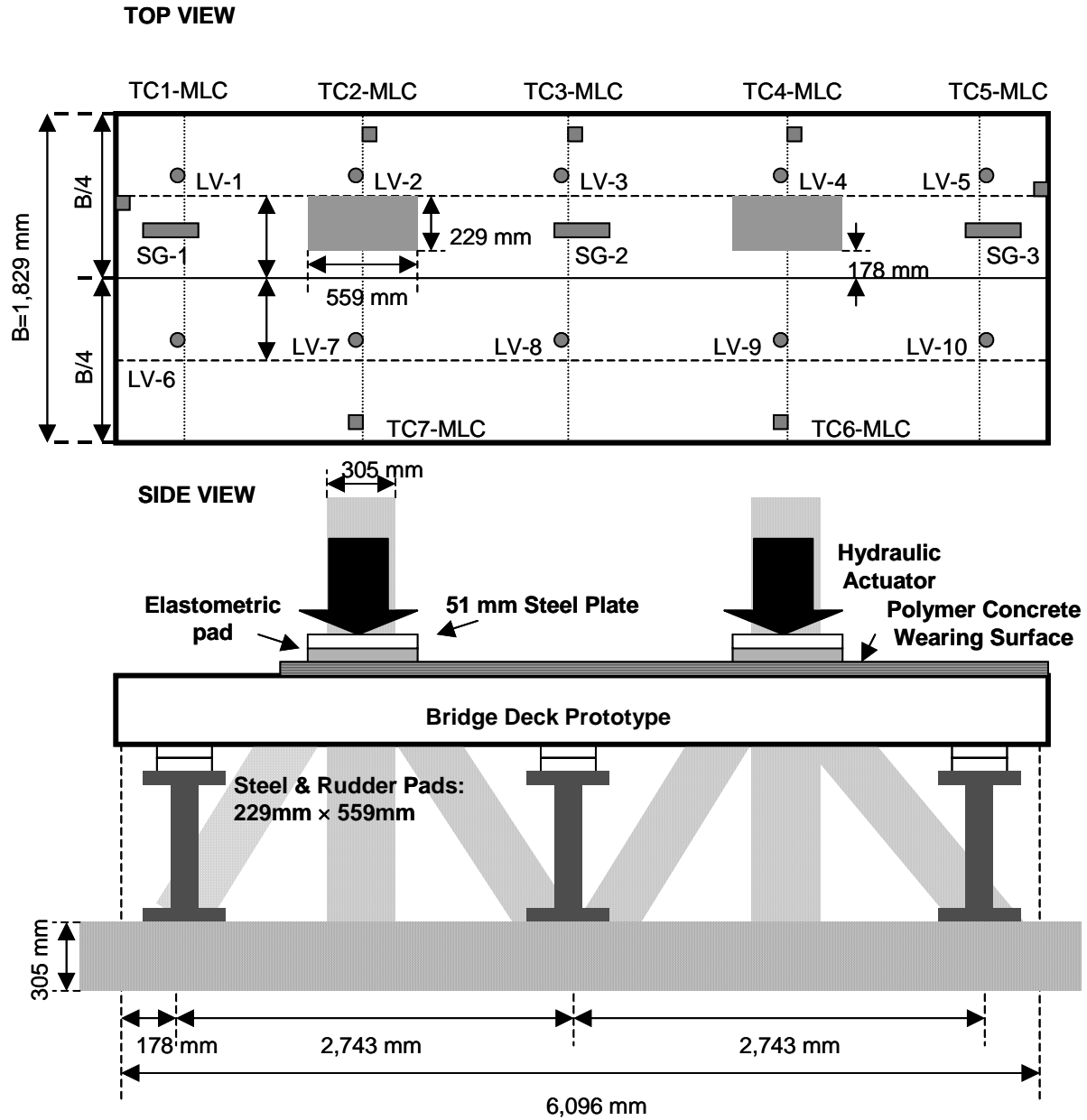


**Figure 5. Test setup and instrumentation layout.**

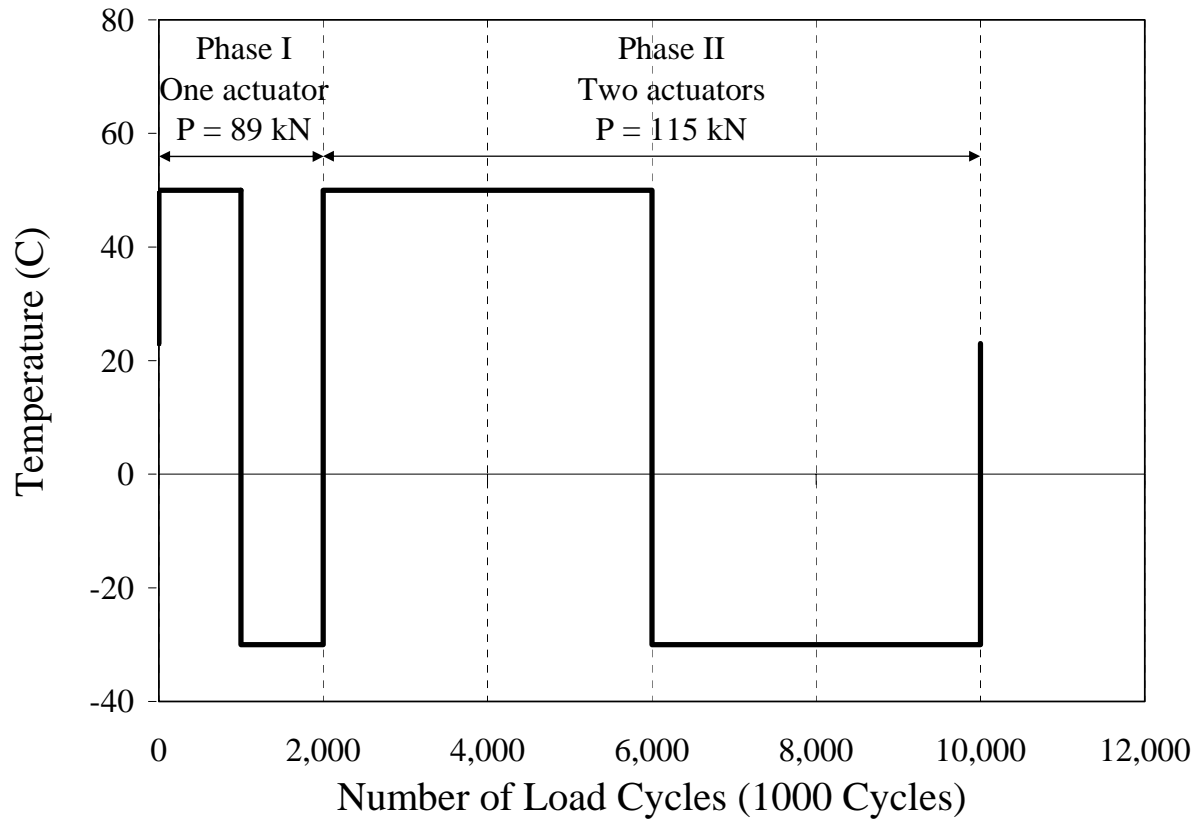


**Figure 6. Load cycling and temperature history.**

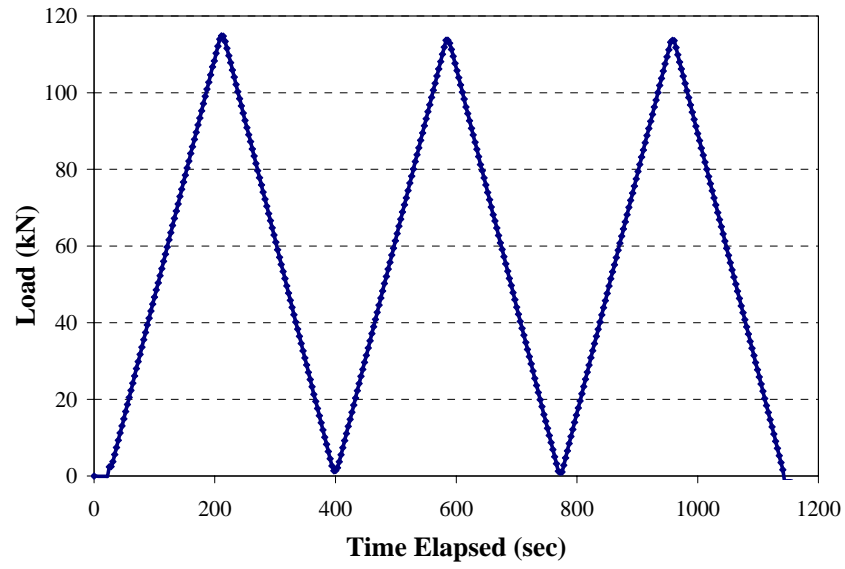
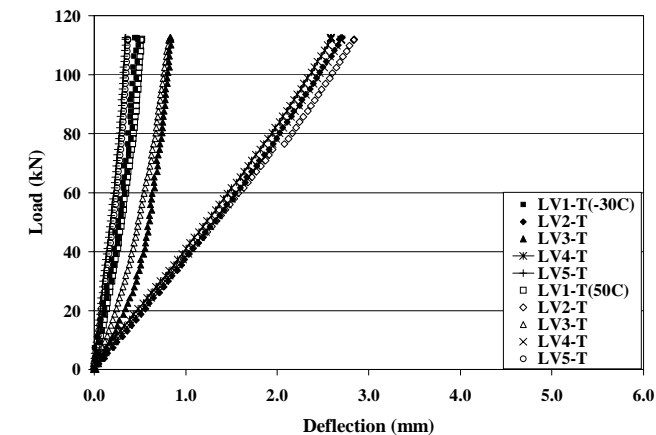
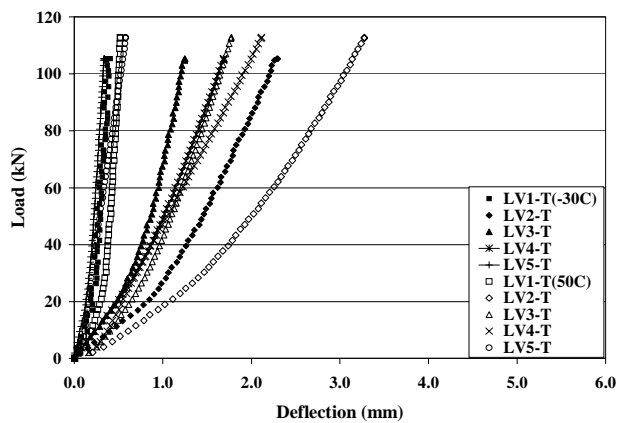


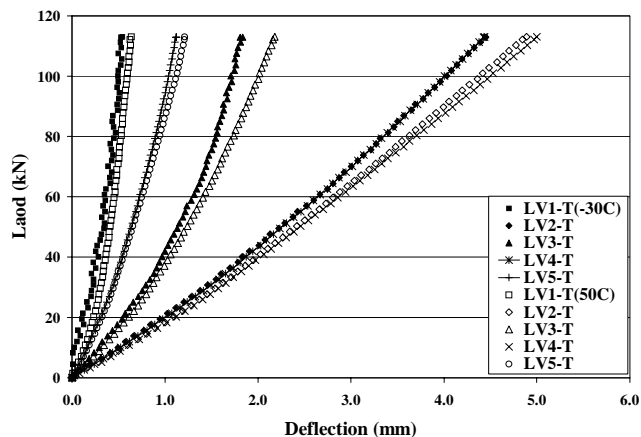
**Figure 7. Typical quasi-static load test**



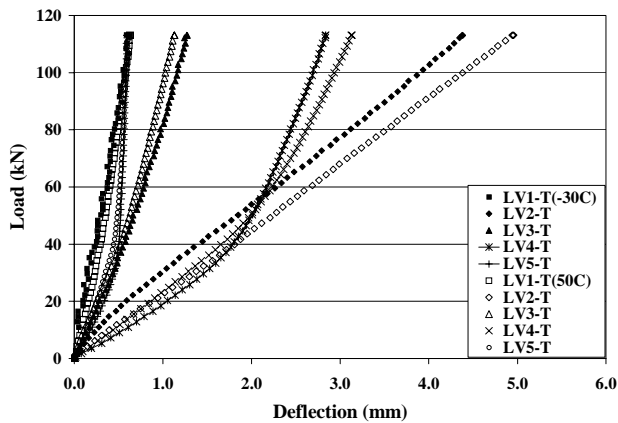
(a)



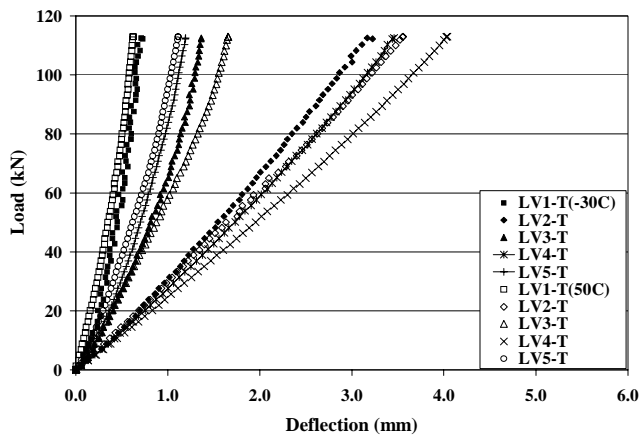
(b)



(c)



(d)



(e)

**Figure 8. Load–deflection curves after ten million cycles of fatigue loading: (a) Bridge #1; (b) Bridge #2; (c) Bridge #3; (d) Bridge #4; (e) Bridge #5**

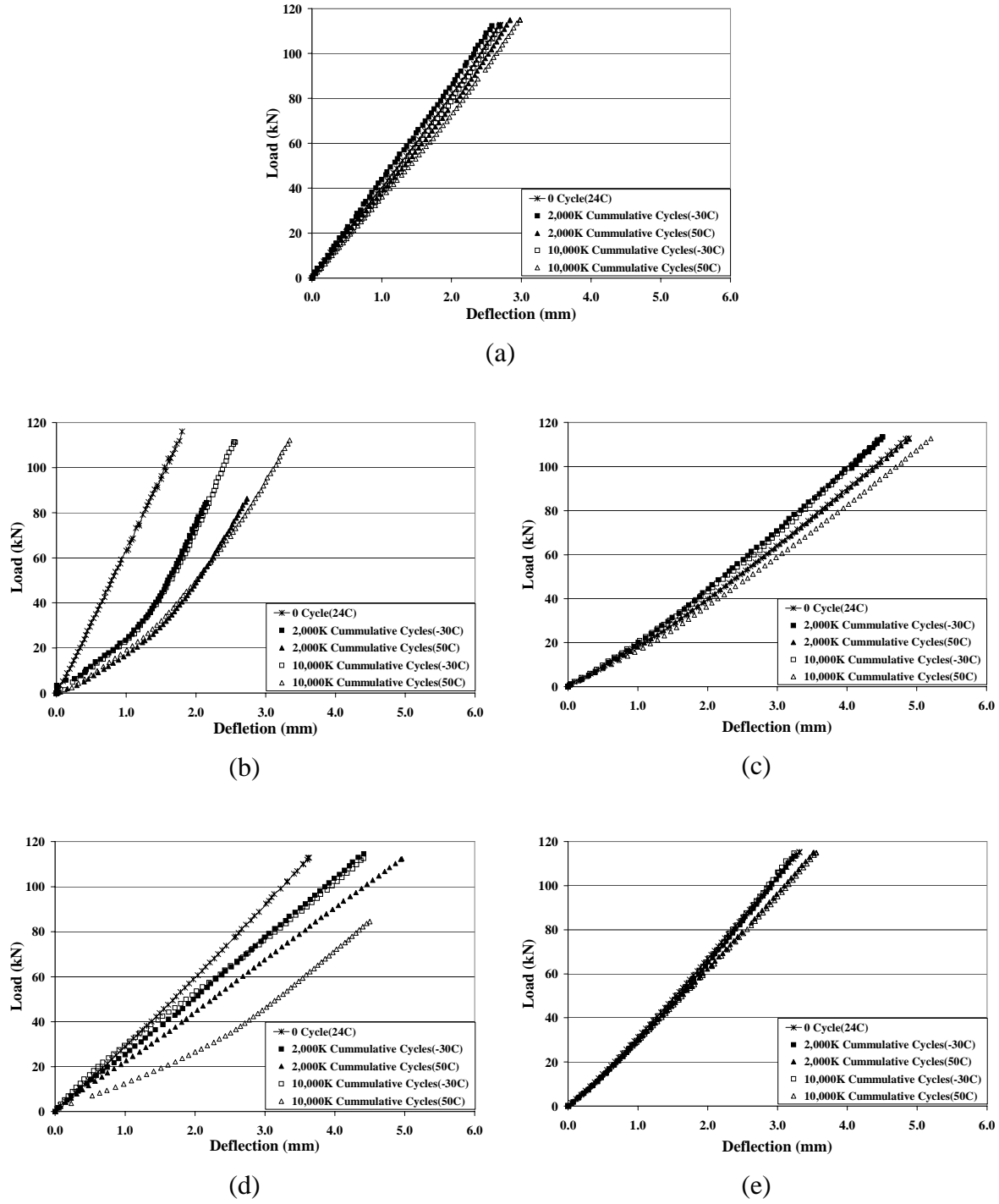


**Figure 9. Load–deflection curves at location LV-2 for increasing load cycles: (a) Bridge #1; (b) Bridge #2; (c) Bridge #3; (d) Bridge #4; (e) Bridge #5**

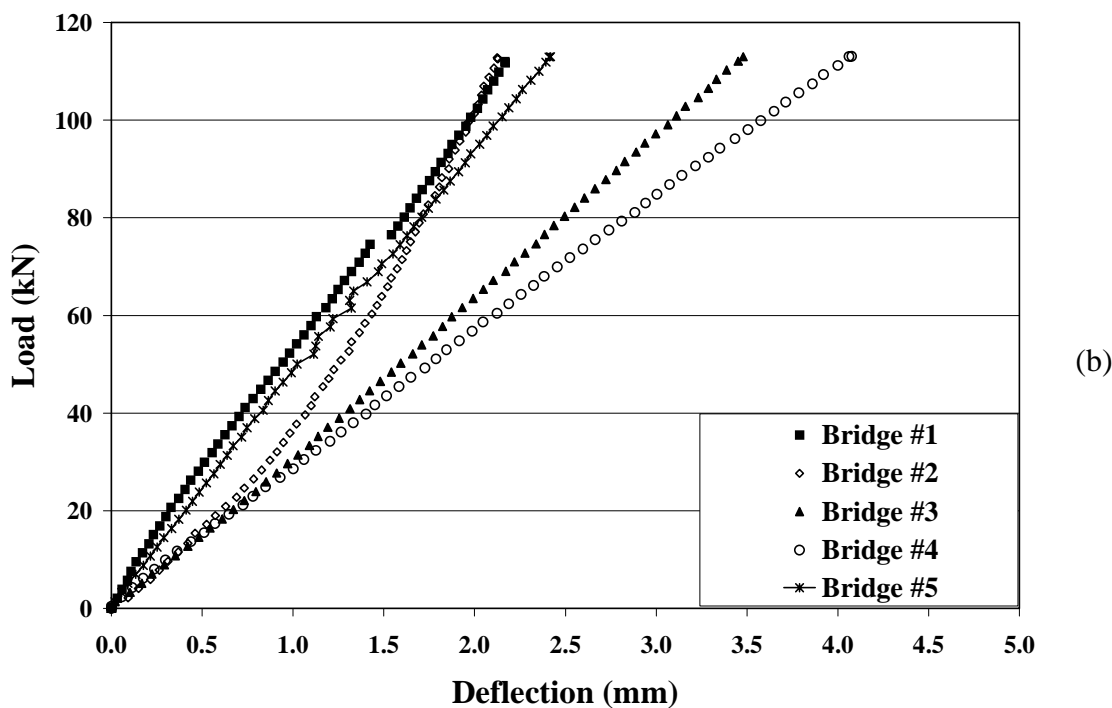
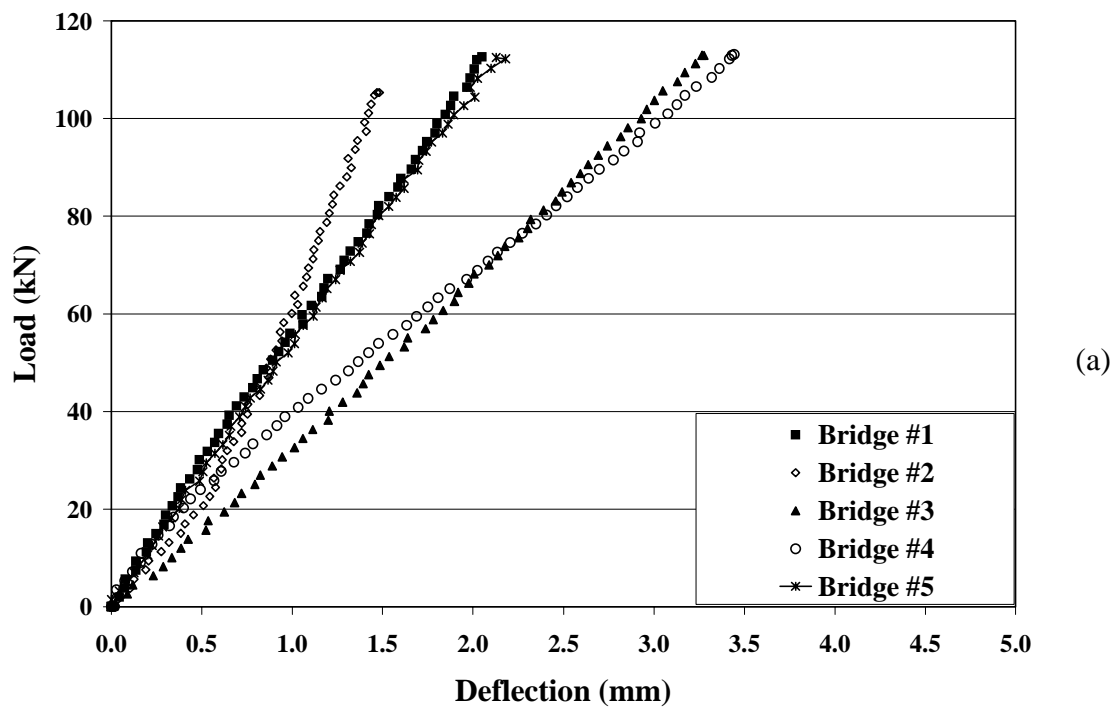


Figure 10. Effects of temperature on the load-deflection response at location LV-2 for 10 million fatigue load cycles: (a) Low temperature; (b) High temperature

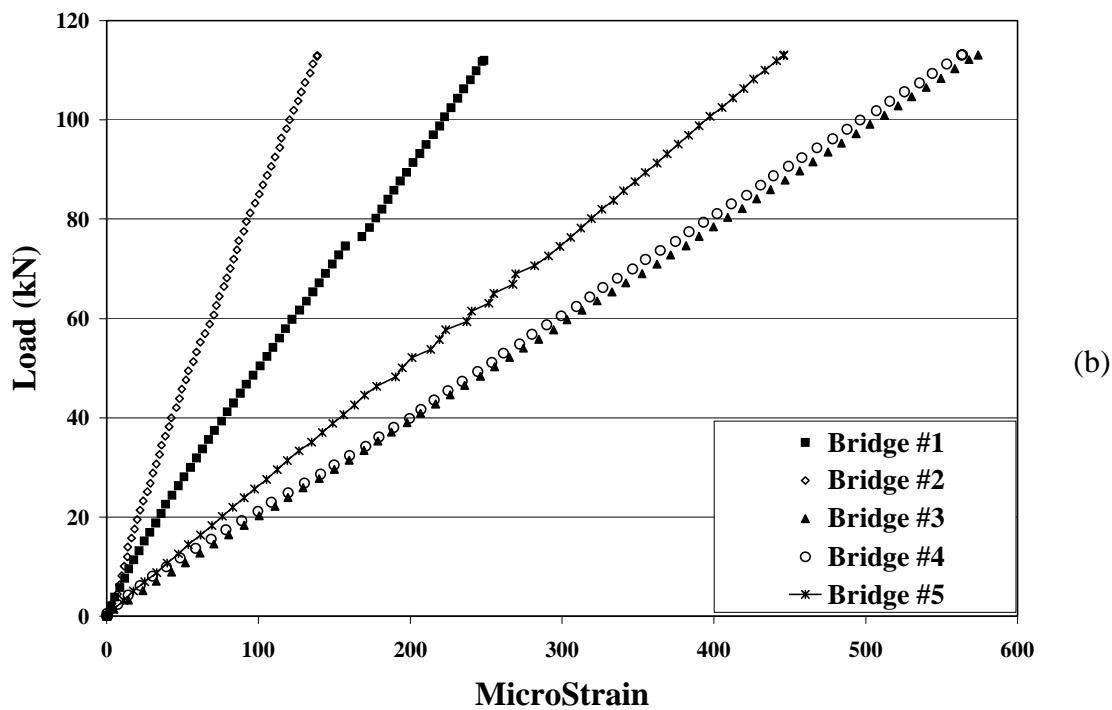
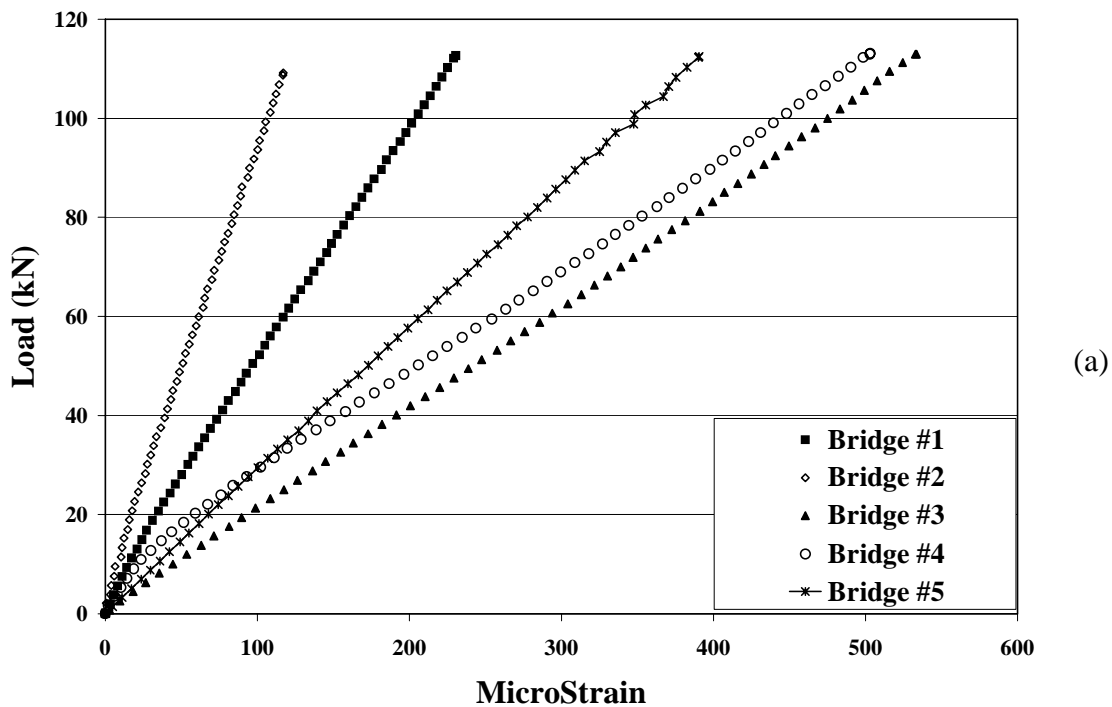
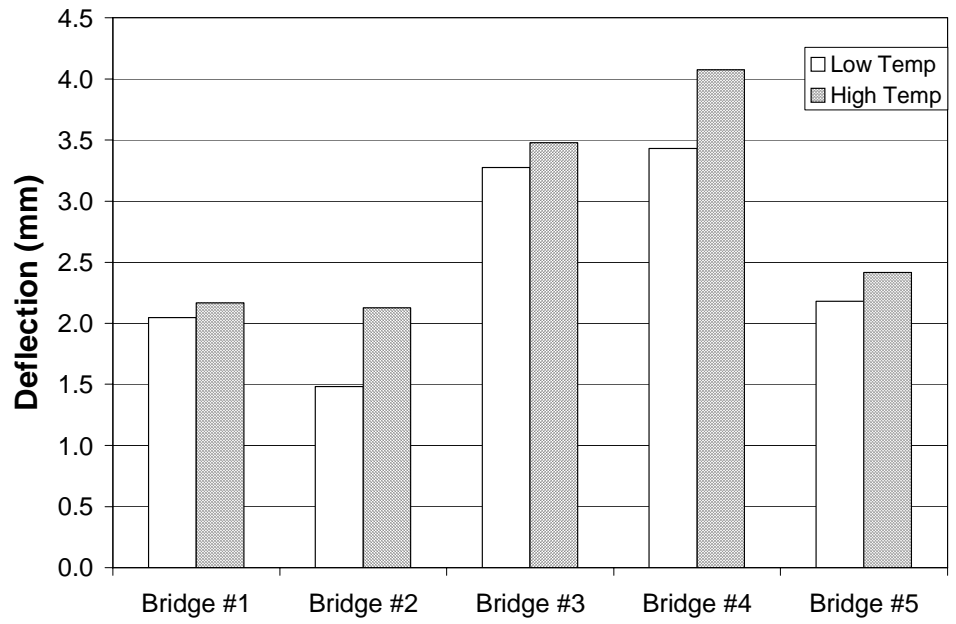
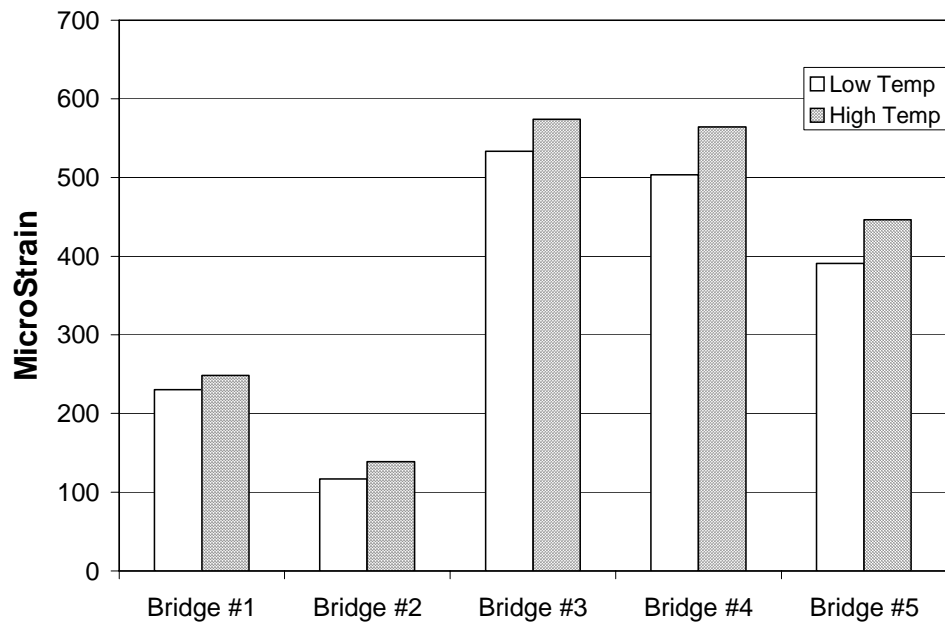


Figure 11. Load–Strain curves for deck prototypes: (a) Low temperature; (b) High temperature



**Figure 12. Comparison of deflections at maximum load after 10 million cycles at location LV-2**



**Figure 13. Comparison of strains at maximum load after 10 million cycles at location SG-2**